

Regional Relationship Between Retinal Nerve Fiber Layer Thickness and Corresponding Visual Field Sensitivity in Glaucomatous Eyes

Akiyasu Kanamori, MD, PhD; Maiko Naka, MD; Azusa Nagai-Kusuhara, MD, PhD; Yuko Yamada, MD, PhD; Makoto Nakamura, MD, PhD; Akira Negi, MD, PhD

Objective: To establish the structure-function relationship between peripapillary retinal nerve fiber layer (RNFL) thickness and visual field (VF) test points in standard automated perimetry.

Methods: We included 213 eyes with open-angle glaucoma and VF loss in this cross-sectional study. Correlations between individual VF sensitivity at 52 test points and peripapillary RNFL thickness divided into 16 sectors were calculated. The RNFL thickness was measured by Stratus optical coherence tomography. A new VF cluster map corresponding to RNFL sectors was generated by grouping the VF test points with the highest relation to each RNFL sector.

Results: The VF sensitivity at each test point was significantly correlated with the sectoral RNFL thickness. The

highest coefficient of determination (R^2) for a superotemporal RNFL sector and VF sensitivity at an inferotemporal test point (9° temporal and 15° inferior from the center) in standard automated perimetry was 0.500 ($P < .001$). Clustered VF test points most highly related to the RNFL sectors were asymmetrically located between the upper and lower hemifields. A newly developed map revealed significant structure-function relationships.

Conclusions: We describe an association between VF sensitivity at test points and sectoral RNFL thickness. Nine clustered VF test points corresponding to 9 RNFL regions were demonstrated from the structure-function relationships.

Arch Ophthalmol. 2008;126(11):1500-1506

GLAUCOMA IS AN OPTIC NEUROPATHY characterized by progressive injury of the optic nerve and retinal nerve fiber layer (RNFL) that results in visual field (VF) deficits.¹ It is of critical importance to detect the relationship between structural (RNFL or optic disc configuration) and functional (VF) damage for the diagnosis and management of glaucomatous optic neuropathy.

Various ocular imaging instruments, such as confocal scanning laser ophthalmoscopy, scanning laser polarimetry, and optical coherence tomography (OCT), have become available. Confocal scanning laser ophthalmoscopy can analyze optic disc configuration, whereas scanning laser polarimetry and OCT can measure RNFL thickness with objectivity and reproducibility.²⁻⁴ In routine clinical practice, the VF is usually assessed via fixed test points with 6° distance with standard automated perimetry (SAP). A recent article claimed that RNFL thickness, measured by Stratus OCT,

showed the strongest structure-function relationship among the 3 instruments.⁵

Gardiner et al⁶ examined the relationships between VF sensitivity (VFS) at 52 tested locations using SAP and optic disc configuration using confocal scanning laser ophthalmoscopy. According to this study, VFS at each test point was significantly correlated with neuroretinal rim narrowing of the optic disc. As another way of analyzing structure and function, dividing the VF by grouping VFS points into several areas and averaging the threshold values of the clustered VFS points was documented. For example, Garway-Heath et al⁷ proposed a map of SAP test locations relating to positions of entry into the optic disc using RNFL defects recorded by photographs. However, to our knowledge there have been no studies evaluating the association of VFS at individual test points or at clustered points with peripapillary RNFL thickness measured with OCT technology.

The purposes of this study are to investigate the relationship between VFS at each

Author Affiliations: Division of Ophthalmology, Department of Surgery, Kobe University Graduate School of Medicine, Kobe, Japan.

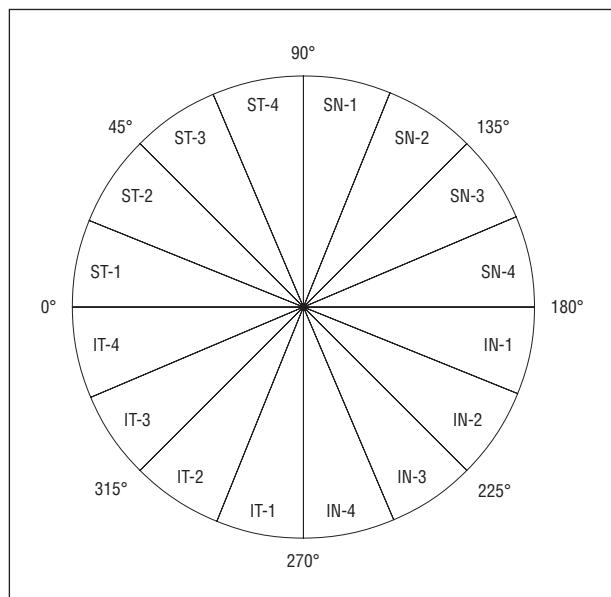


Figure 1. Schematic diagram of 16 retinal nerve fiber layer sectors in right eyes measured with optical coherence tomography. ST indicates superotemporal; SN, superonasal; IN, inferonasal; and IT, inferotemporal.

tested location in SAP and RNFL thickness measured with Stratus OCT and to evaluate the strength of the functional and structural association when the map described by Garway-Heath and colleagues is adopted. In addition, we developed a new structure-function map relating clustered VF test points to RNFL sectors, which is based on the RNFL thickness measured with OCT, and compared the relationships between the 2 maps.

METHODS

In this retrospective study, nonrandomized subjects in the Department of Ophthalmology, Kobe University Hospital, Kobe, Japan, were consulted between April 1, 2005, and November 30, 2006. This study was conducted in accordance with the ethical standards stated in the 1964 Declaration of Helsinki and with the approval of the Medical Ethical Committee of the Kobe University Graduate School of Medicine. The committee determined that this study did not need subjects' approval.

A total of 213 glaucomatous eyes from 131 Japanese adults (66 men and 65 women) younger than 70 years were enrolled in this study. No subjects had a history of diabetes mellitus. All of the eyes underwent comprehensive ophthalmic examinations and had a best-corrected visual acuity of at least 20/40 with spherical refraction of more than -8.0 diopters (D) and cylinder correction within ± 3.0 D. No eyes had closed angle, retinal disease, or significant vitreous opacity. Glaucomatous eyes were defined as those with structural glaucomatous change (vertical cup-disc asymmetry between fellow eyes of ≥ 0.2 , a cup-disc ratio of ≥ 0.6 , and neuroretinal rim narrowing, notches, localized pallor, or RNFL defects) with glaucomatous VF loss in the corresponding hemifield. Glaucomatous VF defects were defined as those with consecutive, repeated abnormal SAP results (≥ 2 contiguous points with a pattern deviation sensitivity loss of $P < .01$, ≥ 3 contiguous points with a sensitivity loss of $P < .05$ in the superior or inferior arcuate areas, a 10-dB difference across the nasal horizontal midline at ≥ 2 adjacent locations, or an abnormal result in the glaucoma hemifield test).

The SAP was performed with the Humphrey Field Analyzer 750 (Humphrey-Zeiss Instruments, Dublin, California) using the Swedish Interactive Threshold Algorithm standard and central 30-2 program. The VF reliability criteria included fixation losses and false-positive and false-negative rates of less than 25%. The SAP and OCT examinations were performed within a maximum period of 3 months.

RNFL THICKNESS

The RNFL thickness was measured with the peripapillary Fast RNFL program of the Stratus OCT (Carl Zeiss Meditec, Inc, Dublin) after a pupillary dilation. The basic principles and technical characteristics of the OCT have been described previously.⁸ The RNFL thickness was calculated using the system software (Stratus version 3.0 software; Carl Zeiss Meditec, Inc). One well-focused scan with a best signal length of at least 7 was included. Images with inappropriate RNFL borders, such as those that penetrated to another layer, were excluded.

The RNFL thickness was determined at 256 circumpapillary points (1.40625°) on a circle with a default diameter of 3.4 mm around the center of the optic disc. The data were exported and then combined into 16 sectors (22.5°) as shown in **Figure 1**. When the temporal margin was designated as 0° , superotemporal sectors 1 through 4 were 0° to 22.5° , 22.5° to 45° , 45° to 67.5° , and 67.5° to 90° , respectively. Superonasal sectors 1 through 4 were 90° to 112.5° , 112.5° to 135° , 135° to 157.5° , and 157.5° to 180° , respectively. Inferonasal sectors 1 through 4 were 180° to 202.5° , 202.5° to 225° , 225° to 247.5° , and 247.5° to 270° , respectively. Inferotemporal sectors 1 through 4 were 270° to 292.5° , 292.5° to 315° , 315° to 337.5° , and 337.5° to 360° , respectively.

STATISTICAL ANALYSES

All of the data were exported into a personal computer. Left-eye data were converted into right-eye format. All of the statistical analyses were performed using StatView version 5.0 statistical software (SAS Institute, Inc, Cary, North Carolina).

The VFS at the 52 nonblind test points located within the 24-2 SAP VF was used and expressed in decibels. The relationships between RNFL thickness in 16 sectoral regions and VFS at the individual 52 points, as well as clusters of VFS as described in detail later, were subjected to a quadratic regression analysis. Second-order polynomial regression analysis has been demonstrated to better fit structure-function relationships than linear analysis when VFS is expressed in a logarithmic form (eg, in decibels), whereas this fit does not hold when VFS is expressed in a nonlogarithmic form (eg, $1/\lambda$ Lambert).^{9,10} The coefficient of determination (R^2) was found by the quadratic regression. $P < .05$ was considered statistically significant.

The structure-function relationships from 6 regions were adopted from the map (**Figure 2**) designated previously by Garway-Heath and colleagues. In addition, a different map of the VFS clusters related to RNFL thickness was generated as follows. The RNFL sector with the highest relationship with VFS at each VF test point was extracted. Based on these data, the contiguous VF test points that had the highest R^2 with an identical RNFL sector could be grouped into a specific area of these contiguous VFS test points. Among the RNFL sectors, superotemporal sectors 1 and 2, inferotemporal sectors 3 and 4, and superonasal sectors 2 to 4 and inferonasal sectors 1 to 3 had significant relationships with a few VF test points. Thus, these 3 regions of RNFL sectors were combined. By doing this, 9 regional areas were constructed as the new map. Correlations between structure-function relationships in the new map were calculated.

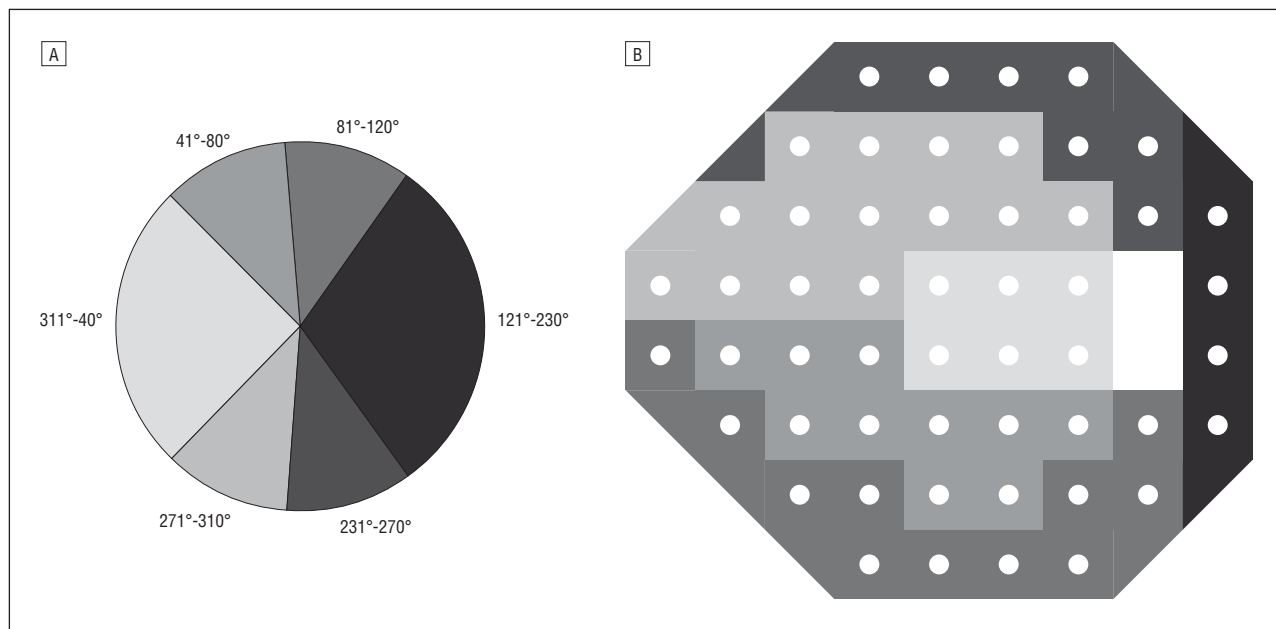


Figure 2. A topographic map generated from Garway-Heath et al.⁷ Areas of the peripapillary retinal nerve fiber layer are divided into 6 sectors (A), and the corresponding visual field regions in standard automated perimetry are shown (B).

RESULTS

The mean (SD) subject age was 51.5 (11.4) years (range, 22-69 years). The mean deviation in SAP ranged from -23.15 to -0.94 dB with a mean (SD) of -6.40 (5.45) dB. The mean (SD) VFS at the 52 nonblind locations in the 24-2 VF was 23.97 (5.57) dB.

The VFS at individual test points was significantly related to the thickness of more than 3 RNFL sectors. Among the 832 (52 × 16) relationships, the highest R^2 was 0.500 between RNFL superotemporal sector 3 and VFS at a test point located 6° temporally and 9° inferiorly from the center. **Figure 3** shows pie charts representing graded R^2 between VFS at individual test points and RNFL sectors allocated according to the 24-2 test point locations. As earlier, each pie corresponds to a defined RNFL sector. The darker a sector is shaded, the stronger the R^2 relationship is. A white sector represents no significant relationship. The RNFL superonasal sector 4 had no significant relationship with VFS at any tested points. When a pair of VFS test points located in the mirror position at the upper and inferior hemifields was compared, the RNFL sector with the highest R^2 tended to be oriented more vertically in the upper hemifield. The highest R^2 at the 52 locations on SAP are shown in **Figure 4**. Overall, VFS in the nasal VF exhibited a higher R^2 than that in the temporal VF.

Figure 5 shows the RNFL sector that had the highest association with VFS at each VF test point from the pie chart shown in **Figure 3**. A bisecting line is drawn at the edge of the circle for each location in the sector corresponding to the entry points of RNFL defect by Garway-Heath and colleagues, and their degrees are shown for comparison with our map. The locations were determined using the temporal margin (9-o'clock position) set as 0° in right eyes. The correspondence rate between the 2 maps was 54% (28 of 52 test points) for the VF test points. The VF test points in nasal retina tend to have

associations with RNFL sectors oriented slightly more toward the temporal side (0°) compared with the map by Garway-Heath and colleagues.

The 52 VF test points were clustered into regional groups of VFs that corresponded to RNFL sectors in 2 ways. First, the arrangement from Garway-Heath and colleagues was adopted (**Figure 2**). Coefficients of determination (R^2) between these 6 VFS clusters and the corresponding 6 sectors are listed in **Table 1**. Second, we generated a different grouped structure-function map that had 9 regional corresponding areas as mentioned in the "Methods" section (**Figure 6**). As shown in **Table 2**, the strength of correspondence between the RNFL sectors and the clustered VF test points in this map was similar to that in the map from Garway-Heath and colleagues in which the association between the sectoral optic disc margin and the clustered VF test points was evaluated. There was an asymmetrical correspondence of the VF loci and RNFL sectors between the upper and lower hemifields.

COMMENT

There were significant correlations between the VFS at individual test points and in several RNFL sectors. Grouping VF test points into 9 areas enabled us to generate the OCT-based structure-function correspondence map. The correspondence was somewhat different from a map generated by Garway-Heath and colleagues. This difference was rooted primarily with regions of structural parameters measured. Garway-Heath and colleagues used the optic disc margin,⁷ whereas OCT measured the RNFL thickness away from the optic disc margin. Because retinal nerve fibers do not project radially from the optic disc, the retinotopic orientation is different between a site on the optic disc margin and that on the concentric RNFL.

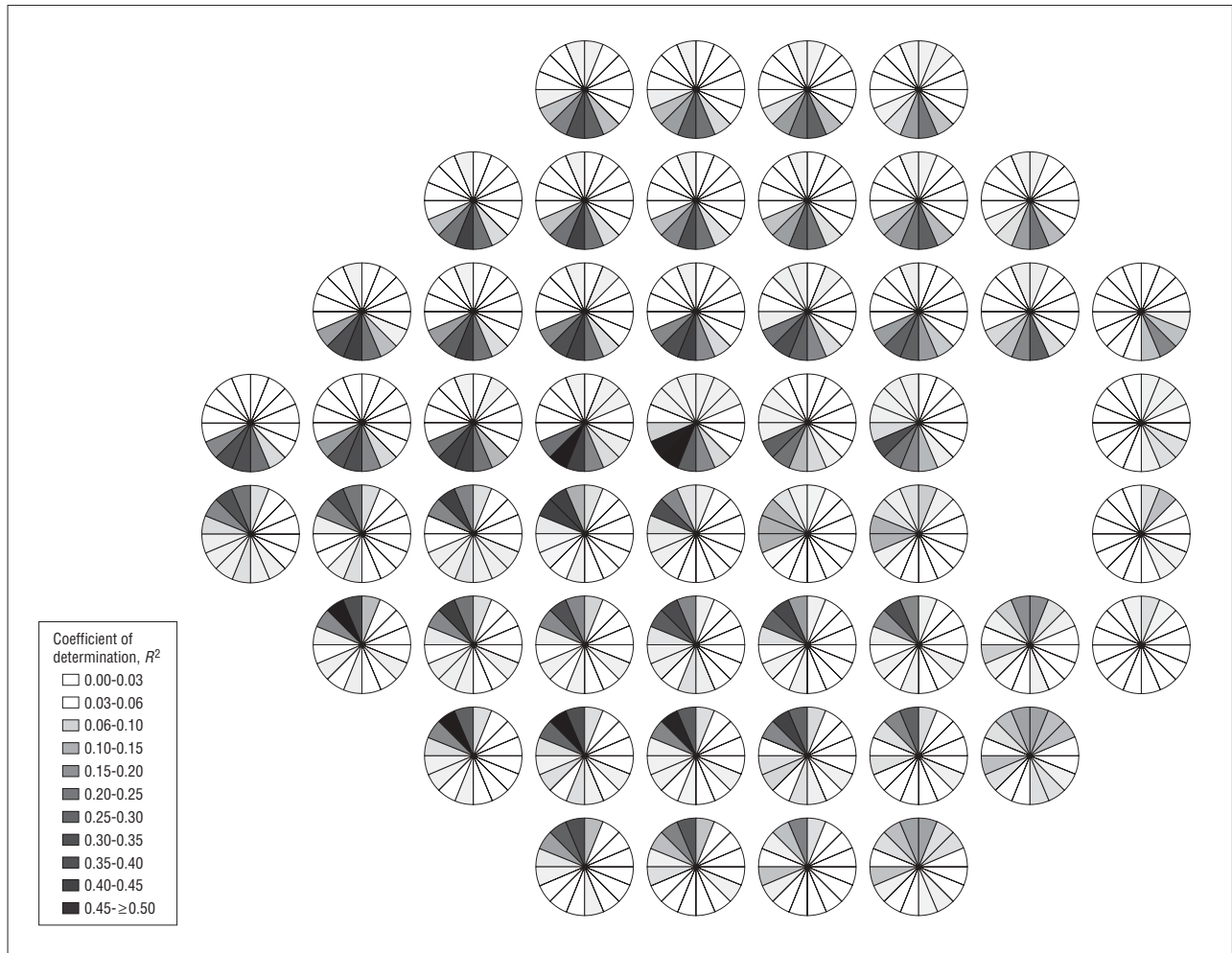


Figure 3. The relationship between retinal nerve fiber layer sectors and visual field sensitivity at 52 test points in standard automated perimetry with a 24-2 central program. Each circle shows the relation map for 1 test point in the visual field. The retinal nerve fiber layer sectors are shaded according to the strength of the correlation of determination (R^2), with darker shading indicating a larger correlation.

On the other hand, both maps show an asymmetrical correspondence of VFS loci and RNFL sectors between the upper and lower hemifields. Inferior RNFL sectors govern broader VF clusters in the upper hemifield than superior RNFL sectors in the lower hemifield. A previous investigation¹¹ using a cluster analysis of static VFs described horizontal asymmetry. Another study¹² also showed horizontal asymmetry in the long-term progression of glaucomatous VF loss. Duke-Elder¹³ noticed the asymmetry in the entry of ganglion cell axons into the optic disc. He noted that axons from the inferior retina preferentially entered into the nasal side of the optic disc more frequently than those from the upper retina. From another point of view, clockwise rotation in the right eye and counterclockwise rotation in the left eye can be used to describe RNFL sector orientation relative to VF loci. Similar asymmetry of the structure-function relationships was also demonstrated in a previous study² that analyzed optic disc configuration by confocal scanning laser ophthalmoscopy and a recent study¹⁴ that analyzed RNFL thickness by Stratus OCT. The degree of rotation in our map may consist of more than

					0.355	0.335	0.322	0.291				
					<.0001	<.0001	<.0001	<.0001				
					0.410	0.439	0.390	0.304	0.308	0.280		
					<.0001	<.0001	<.0001	<.0001	<.0001	<.0001		
					0.475	0.438	0.440	0.413	0.379	0.320	0.302	0.244
					<.0001	<.0001	<.0001	<.0001	<.0001	<.0001	<.0001	<.0001
					0.433	0.398	0.444	0.460	0.498	0.328	0.353	0.083
					<.0001	<.0001	<.0001	<.0001	<.0001	<.0001	<.0001	<.001
					0.377	0.363	0.423	0.364	0.350	0.192	0.169	0.102
					<.0001	<.0001	<.0001	<.0001	<.0001	<.0001	<.0001	<.0001
					0.477	0.407	0.398	0.433	0.319	0.387	0.232	0.093
					<.0001	<.0001	<.0001	<.0001	<.0001	<.0001	<.0001	<.0001
					0.455	0.500	0.447	0.434	0.316	0.199		
					<.0001	<.0001	<.0001	<.0001	<.0001	<.0001		
					0.362	0.254	0.216	0.197				
					<.0001	<.0001	<.0001	<.0001				

Figure 4. The highest correlations of determination between visual field sensitivity and sectoral retinal nerve fiber layer thickness at 52 tested locations. P values are also shown.

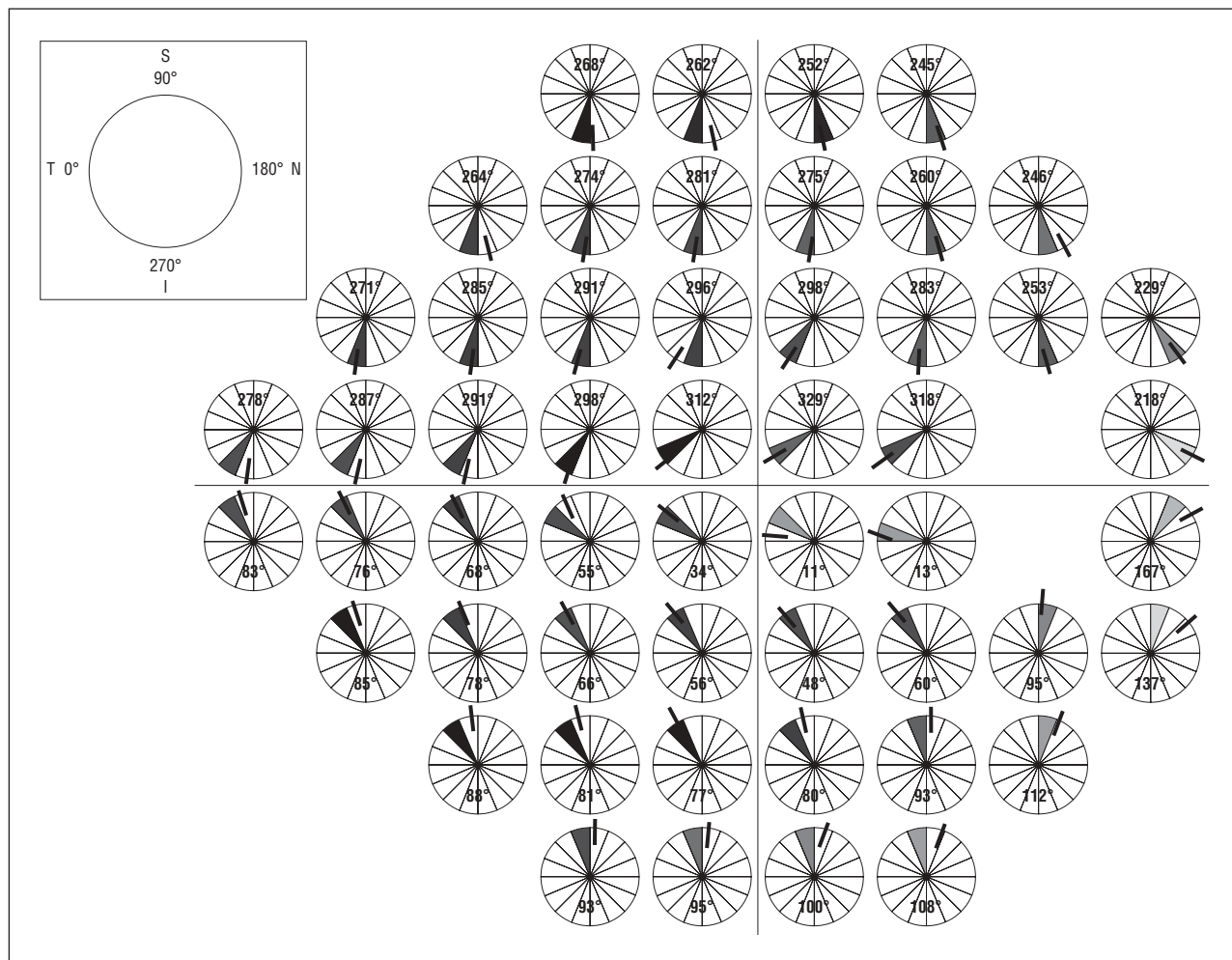


Figure 5. The retinal nerve fiber layer sector most highly correlated with visual field sensitivity at each test location as shaded in Figure 3. Bisecting lines at the edge of the circle and their degrees for each location in the sector corresponding to retinal nerve fiber layer defect by the map from Garway-Heath et al⁷ are shown. S indicates superior; N, nasal; I, inferior; and T, temporal.

Table 1. Structure-Function Relationships in the Map by Garway-Heath and Colleagues^a

Sector in RNFL	Correlation of Determination, R^2
Temporal, 311°-40°	0.34
Superotemporal, 41°-80°	0.53
Superonasal, 81°-120°	0.20
Nasal, 121°-230°	0.08
Inferonasal, 231°-270°	0.28
Inferotemporal, 271°-310°	0.51

Abbreviation: RNFL, retinal nerve fiber layer.

^aThe map is from Garway-Heath et al.⁷ All of the associations are $P < .001$.

1 RNFL sector (equal to 22.5°). Garway-Heath and colleagues demonstrated that the location of the optic nerve head was a mean (SD) of 15.5° (0.9°) nasal to and 1.9° (1.0°) above the fovea. It could be speculated that the rotation angle was 7.0° (tangent $7 = 1.9/15.5$) from their data. Another study¹⁵ reported this angle to be 5.6°. We suggest that the degree of rotation in our map is bigger than that of the anatomical rotation. Whether this asymmetry affects or is responsible for the develop-

ment and progression of glaucomatous optic neuropathy is a matter of particular interest and requires further investigation.

The R^2 values at VF locations temporal to the blind spot were relatively low compared with those at locations nasal to the blind spot. Additionally, the superonasal sector 4 of the RNFL showed no significant relationship with VFS at any tested location in SAP. These results may arise owing to the small number of eyes with low VFS in this area. Only 6 of 213 eyes (2.8%) had a VFS less than 10 dB at the test point 6° temporal to the blind spot, whereas 31 of 213 eyes (14.6%) had a VFS less than 10 dB at the test point 6° nasal to the blind spot. It has been suggested that the thickness of the nasal RNFL sector has higher individual variability and less reproducibility.¹⁶ It is very difficult to estimate the structure-function relationship at the nasal area adjacent to the optic disc because of the paucity of test points on SAP at the temporal regions adjacent to the blind spot.

There are several limitations to this type of study. First, there may be a selection bias. In this study, glaucoma was defined on the basis of structure and VF loss. We wanted to generate a corresponding map between OCT-based RNFL thickness and VF test points. To facilitate this procedure,

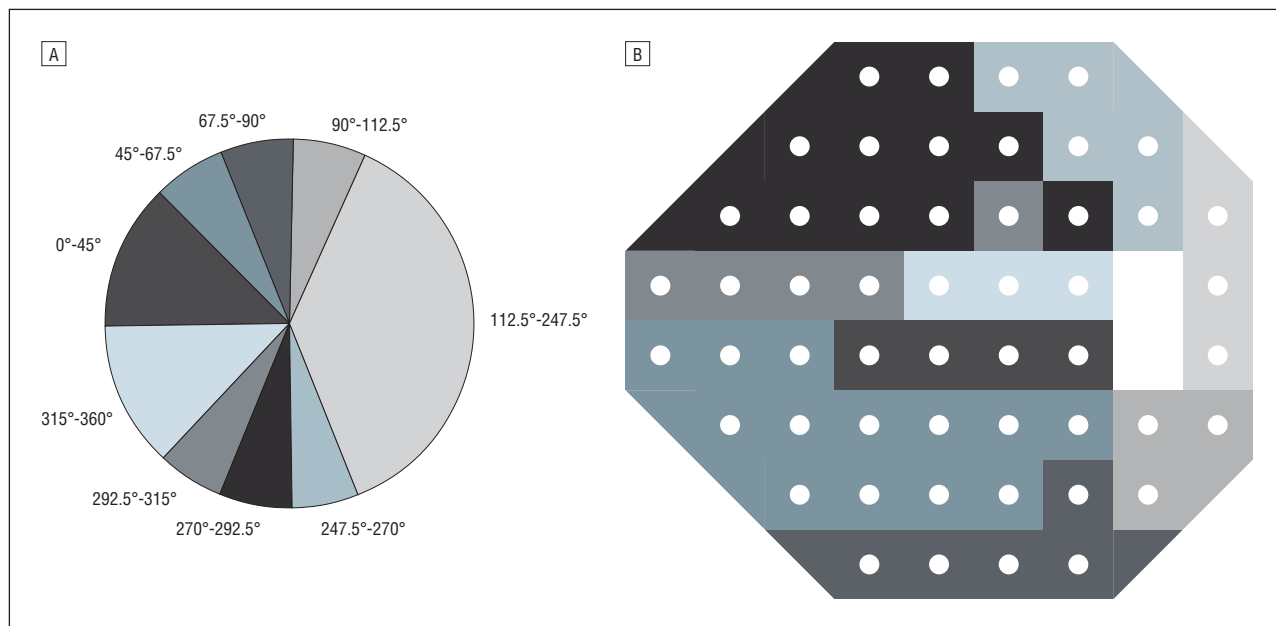


Figure 6. A new topographic map generated from data in this study. Areas of the peripapillary retinal nerve fiber layer are divided into 9 sectors (A), and the corresponding visual field regions in standard automated perimetry are shown (B).

Table 2. Structure-Function Relationships in Our Map^a

Sector in RNFL	Correlation of Determination, R^2
Temporal ST, 0°-45°	0.30
Middle ST, 45°-67.5°	0.54
Superior ST, 67.5°-90°	0.35
Superonasal, 90°-112.5°	0.21
Nasal, 112.5°-247.5°	0.16
Inferonasal, 247.5°-270°	0.35
Inferior IT, 270°-292.5°	0.48
Middle IT, 292.5°-315°	0.48
Temporal IT, 315°-360°	0.40

Abbreviations: IT, inferotemporal; RNFL, retinal nerve fiber layer; ST, superotemporal.

^aAll of the associations are $P < .0001$.

we intentionally used eyes with glaucomatous optic neuropathy with VF loss. Therefore, eyes with so-called preperimetric glaucomatous optic neuropathy were excluded from this study. This may cause some bias in establishing the strength of the structure-function associations.

Second, we included both eyes in the partial population. It is known that optical and biochemical characteristics are similar between bilateral eyes. The use of both eyes may therefore inflate the structure-function association values.

Third is the aging effect. Because RNFL thickness measured by OCT is known to be significantly reduced in eyes from an older population,^{17,18} participants older than 70 years were excluded. Additionally, we reported that RNFL thickness was affected by both the size of the optic disc and refraction.¹⁹ We cannot completely rule out the influence of these issues on the present results because corrected measurements (eg, total deviation at tested locations in SAP or age-adjusted RNFL thickness) were not used.

Last but not least, the structure-function relationship may be skewed. The range of defect depth at specific VF test points affects the strength of the associations. If there is greater loss in some RNFL or VF locations, this may result in a stronger apparent association with these locations even if the true association is with correlated but less damaged RNFL or VF locations. Also, if some RNFL sectors tend to have less interindividual variability than others, the apparent (statistical) association may be stronger with a correlated but less variable RNFL sector. This may distort the true structure-function relationship. These effects may skew associations to the inferotemporal and superotemporal (arcuate) regions of the RNFL. As reviewed by Hood and Kardon,²⁰ the actual correspondence between structure and function cannot be fully revealed.

In conclusion, the OCT-measured sectoral RNFL thickness had significant associations with VFS on SAP. The correspondence map between clustered VF test points and the grouped RNFL sectors was different from the map proposed by Garway-Heath and colleagues, essentially owing to differences of measurement of structural parameters. Both maps showed an asymmetrical correspondence of VFS loci and RNFL sectors between the upper and lower hemifields.

Submitted for Publication: October 18, 2007; final revision received June 25, 2008; accepted June 28, 2008.

Correspondence: Akiyasu Kanamori, MD, PhD, Division of Ophthalmology, Department of Surgery, Kobe University Graduate School of Medicine, 7-5-2 Kusunokicho, Chuo-ku, Kobe 650-0017, Japan (kanaaki@med.kobe-u.ac.jp).

Financial Disclosure: None reported.

Funding/Support: This study was supported by grants 19791267 (Dr Kanamori), 17591835 (Dr Nakamura), and 19390444 (Drs Kanamori, Nakamura, and Negi) from the

Ministry of Education, Culture, Sports, Science, and Technology of the Japanese Government and the Imai Memorial Foundation for Glaucoma Research (Dr Kanamori). **Previous Presentation:** This paper was presented as a poster at the annual meeting of the American Academy of Ophthalmology; November 11, 2007; New Orleans, Louisiana.

REFERENCES

1. Weinreb RN, Khaw PT. Primary open-angle glaucoma. *Lancet*. 2004;363(9422):1711-1720.
2. Cioffi GA, Robin AL, Eastman RD, Perell HF, Sarfarazi FA, Kelman SE. Confocal laser scanning ophthalmoscope: reproducibility of optic nerve head topographic measurements with the confocal laser scanning ophthalmoscope. *Ophthalmology*. 1993;100(1):57-62.
3. Schuman JS, Pedut-Kloizman T, Hertzmark E, et al. Reproducibility of nerve fiber layer thickness measurements using optical coherence tomography. *Ophthalmology*. 1996;103(11):1889-1898.
4. Hoh ST, Ishikawa H, Greenfield DS, Liebmann JM, Chew SJ, Ritch R. Peripapillary nerve fiber layer thickness measurement reproducibility using scanning laser polarimetry. *J Glaucoma*. 1998;7(1):12-15.
5. Bowd C, Zangwill LM, Medeiros FA, et al. Structure-function relationships using confocal scanning laser ophthalmoscopy, optical coherence tomography, and scanning laser polarimetry. *Invest Ophthalmol Vis Sci*. 2006;47(7):2889-2895.
6. Gardiner SK, Johnson CA, Cioffi GA. Evaluation of the structure-function relationship in glaucoma. *Invest Ophthalmol Vis Sci*. 2005;46(10):3712-3717.
7. Garway-Heath DF, Poinosawmy D, Fitzke FW, Hitchings RA. Mapping the visual field to the optic disc in normal tension glaucoma eyes. *Ophthalmology*. 2000;107(10):1809-1815.
8. Hee MR, Izatt JA, Swanson EA, et al. Optical coherence tomography of the human retina. *Arch Ophthalmol*. 1995;113(3):325-332.
9. Garway-Heath DF, Caprioli J, Fitzke FW, Hitchings RA. Scaling the hill of vision: the physiological relationship between light sensitivity and ganglion cell numbers. *Invest Ophthalmol Vis Sci*. 2000;41(7):1774-1782.
10. Leung CK, Chong KK, Chan WM, et al. Comparative study of retinal nerve fiber layer measurement by StratusOCT and GDx VCC, II: structure/function regression analysis in glaucoma. *Invest Ophthalmol Vis Sci*. 2005;46(10):3702-3711.
11. Schlottmann PG, De Cilla S, Greenfield DS, Caprioli J, Garway-Heath DF. Relationship between visual field sensitivity and retinal nerve fiber layer thickness as measured by scanning laser polarimetry. *Invest Ophthalmol Vis Sci*. 2004;45(6):1823-1829.
12. Pereira ML, Kim CS, Zimmerman MB, Alward WL, Hayreh SS, Kwon YH. Rate and pattern of visual field decline in primary open-angle glaucoma. *Ophthalmology*. 2002;109(12):2232-2240.
13. Duke-Elder S. *Textbook of Ophthalmology*. Vol 1. St Louis, MO: CV Mosby; 1932.
14. Ferreras A, Pablo LE, Garway-Heath DF, Fogagnolo P, García-Feijoo J. Mapping standard automated perimetry to the peripapillary retinal nerve fiber layer in glaucoma. *Invest Ophthalmol Vis Sci*. 2008;49(7):3018-3025.
15. Rohrschneider K. Determination of the location of the fovea on the fundus. *Invest Ophthalmol Vis Sci*. 2004;45(9):3257-3258.
16. Budenz DL, Chang RT, Huang X, Knighton RW, Tielsch JM. Reproducibility of retinal nerve fiber thickness measurements using the stratus OCT in normal and glaucomatous eyes. *Invest Ophthalmol Vis Sci*. 2005;46(7):2440-2443.
17. Kanamori A, Escano MF, Eno A, et al. Evaluation of the effect of aging on retinal nerve fiber layer thickness measured by optical coherence tomography. *Ophthalmologica*. 2003;217(4):273-278.
18. Budenz DL, Anderson DR, Varma R, et al. Determinants of normal retinal nerve fiber layer thickness measured by Stratus OCT. *Ophthalmology*. 2007;114(6):1046-1052.
19. Nagai-Kusuhara A, Nakamura M, Fujioka M, Tatsumi Y, Negi A. Association of retinal nerve fibre layer thickness measured by confocal scanning laser ophthalmoscopy and optical coherence tomography with disc size and axial length. *Br J Ophthalmol*. 2008;92(2):186-190.
20. Hood DC, Kardon RH. A framework for comparing structural and functional measures of glaucomatous damage. *Prog Retin Eye Res*. 2007;26(6):688-710.